Crystal Structure of Extended-Spectrum β-Lactamase Toho-1: Insights into the Molecular Mechanism for Catalytic Reaction and Substrate Specificity Expansion[†,‡]

Akiko Shimizu Ibuka,*[,§] Yoshikazu Ishii,[||] Moreno Galleni,[⊥] Masaji Ishiguro,[#] Keizo Yamaguchi,[||] Jean-Marie Frère,[⊥] Hiroshi Matsuzawa,[▽] and Hiroshi Sakai[§]

Department of Food and Nutritional Sciences, University of Shizuoka, 52-1 Yada, Shizuoka 422-8526, Japan, Department of Microbiology, Toho University School of Medicine, 5-21-16 Omori-Nishi, Ota-ku, Tokyo 143-8540, Japan, Laboratoire d'Enzymologie, Centre for Protein Engineering, Université de Liège, 4000 Liège, Belgium, Suntory Institute for Bioorganic Research, Wakayamadai, Shimamoto-cho, Mishima-gun, Osaka 618-8503, Japan, and Department of Bioscience and Biotechnology, Aomori University, 2-3-1 Kohbata, Aomori 030-0943, Japan

Received February 19, 2003; Revised Manuscript Received June 17, 2003

ABSTRACT: The crystallographic structure of the class A β-lactamase Toho-1, an extended-spectrum β-lactamase with potent activity against expanded-spectrum cephems, has been determined at 1.65 Å resolution. The result reveals that the Lys73 side chain can adopt two alternative conformations. The predominant conformation of Lys73 is different from that observed in the E166A mutant, indicating that removal of the Glu166 side chain changes the conformation of the Lys73 side chain and thus the interaction between Lys73 and Glu166. The Lys73 side chain would play an important role in proton relay, switching its conformation from one to the other depending on the circumstances. The electron density map also implies possible rotation of Ser237. Comparison of the Toho-1 structure with the structure of other class A β-lactamases shows that the hydroxyl group of Ser237 is likely to rotate through interaction with the carboxyl group of the substrate. Another peculiarity is the existence of three sulfate ions positioned in or near the substrate-binding cavity. One of these sulfate ions is tightly bound to the active center, while the other two are held by a region of positive charge formed by two arginine residues, Arg274 and Arg276. This positively charged region is speculated to represent a pseudo-binding site of the β-lactam antibiotics, presumably catching the methoxyimino group of the third-generation cephems prior to proper binding in the substrate-binding cleft for hydrolysis. This high-resolution structure, together with detailed kinetic analysis of Toho-1, provides a new hypothesis for the catalytic mechanism and substrate specificity of Toho-1.

The most common mechanism of bacterial resistance to β-lactam antibiotics is the production of β-lactamases, enzymes that hydrolyze the amide group of the β-lactam ring to inactivate β-lactams. β-Lactamases are classified into four classes, A, B, C, and D, according to amino acid sequence and substrate specificity (*1*, *2*). This classification separates serine β-lactamases (in which a hydroxyl group of a serine residue is acylated by β-lactams) into classes A, C, and D, while zinc metallo-β-lactamases are grouped into class B. Class A enzymes are most frequently encountered in clinical isolates, often being encoded by genes located on transferable plasmids and exhibiting diverse substrate profiles. These class A enzymes were originally labeled as penicillinases on the basis of their substrate specificity; however, the number of class A enzymes with activity to hydrolyze expanded-spectrum cephalosporins has increased dramatically as clinical use of new β-lactam antibiotics increased (*1*, *3*). These class A β-lactamases with expanded-spectrum substrate specificity are known as extended-spectrum β-lactamases (ESBLs)[1] and are further classified into two subgroups. The largest subgroup is that of non-ESBL derivatives, the extended-spectrum activity of which is the result of a few point mutations in penicillinases such as TEM-1 and SHV-1 (*4*). A large number of TEM and SHV variants have been identified, and their molecular evolution is a point of great interest (*5*−*8*). The other subgroup includes novel ESBLs distantly related to the previously identified class A β-lactamases. This subgroup includes a cluster of enzymes known as CTX-M-type β-lactamases, where the designation CTX refers to their powerful spectrum for hydrolysis of cefotaxime (*9*). These enzymes have unique amino acid sequences, with 70% or higher identity within this subgroup, yet exhibit only 40% or less identity with other class A β-lactamases, indicating that their activity to hydrolyze expanded-spectrum

[†] This work was supported by a grant from the Ministry of Health, Labor, and Welfare of Japan during 2000−2002 (Scientific Research Foundation on Drug Resistant Bacteria), a grant from the Japan Health Science Foundation, a grant from the Society of Japanese Pharmacopooeia, Shionogi & Co., Ltd., and Toho University Project Research Grants 12-20 and 13-12.

[‡] The atomic coordinates of Toho-1 have been deposited in the Protein Data Bank with the entry code 1iys.

* To whom correspondence should be addressed. Tel: +81-54-264-5578. Fax: +81-54-264-5099. E-mail: ibuka@u-shizuoka-ken.ac.jp.

[§] University of Shizuoka.

[||] Toho University School of Medicine.

[⊥] Université de Liège.

[#] Suntory Institute for Bioorganic Research.

[▽] Aomori University.

[1] Abbreviations: ESBL, extended-spectrum β-lactamase; PEG, poly(ethylene glycol); ND, not determined.

10.1021/bi0342822 CCC: $25.00
Published on Web 08/21/2003

cephalosporins is an intrinsic enzymatic property of this subgroup and not the result of point mutations. The number of the reported CTX-M-type enzymes has been increasing, signifying their explosive spread over the world (*9*−*15*).

Toho-1 is an ESBL encoded by a plasmid and produced in *Escherichia coli* TUH12191 isolated from the urine of a patient treated with β-lactam antibiotics (*10*). Toho-1 is classified into the CTX-M group on the basis of its substrate profile and amino acid sequence and belongs to the 2be group according to the functional classification proposed by Bush et al. (*16*). Here we present the crystal structure of wild-type Toho-1 at 1.65 Å resolution. Although impeded by the strong tendency of the wild-type Toho-1 to form twinned crystals, structural analysis was finally achieved through successful preparation of single crystals suitable for X-ray analysis. The high-resolution structure and precise kinetic analysis provide insights into the catalytic mechanism and extended substrate profile of this enzyme.

MATERIALS AND METHODS

Enzyme Preparation. The gene for Toho-1 was cloned and sequenced by a method described previously (*10*). The DNA segment coding for the mature enzyme was inserted into the plasmid vector pET-9a (Novagen) to construct pET-bla for overexpression. *E. coli* BL21(DE3)pLysS [F^- *dcm omp*T *hsd*S_B ($r_B^-m_B^-$) *gal* λ(DE3) pLysS(Cam^r)] transformed with the plasmid pET-bla was cultured in 2-TY broth at 30 °C for 8 h. Expression of the Toho-1 gene was induced with 0.1 mM isopropyl α-D-thiogalactopyranoside. Cells were harvested by centrifugation and then disrupted by sonication. The enzyme in the supernatant was purified by ion-exchange chromatography on a CM-Toyopearl column (Tosoh, Japan) in 20 mM MES buffer (pH 6.5) and eluted with a 0−0.15 M linear NaCl gradient. The purity of the enzyme was assessed to be more than 95% by Coomassie blue staining after SDS−polyacrylamide gel electrophoresis.

Crystal Preparation and Data Collection. The purified protein was dialyzed against 5 mM Tris-HCl buffer (pH 7.0) and concentrated to 10 mg/mL for crystallization. The crystals were prepared by hanging drop or sitting drop vapor diffusion with a reservoir solution of 1.9−2.0 M ammonium sulfate (no other reagents) at 15−20 °C. Triangular pyramidal crystals suitable for X-ray analysis were obtained within about 1 month. As the crystals tended to twin during crystallization, we made efforts to obtain single crystals as follows: (i) the expression vector was modified to produce mature Toho-1 β-lactamase with no signal sequence, (ii) elution from the CM-Toyopearl column was performed with a slower gradient in the purification process, and (iii) finally at the time of data collection, many crystals were rigorously sorted to find single crystals that diffract to higher resolution. X-ray diffraction data were collected using the 6A beamline of the High Energy Accelerator Research Organization (KEK, Tsukuba, Japan) at 100 K with a Mar charge-coupled device (CCD) detector. The crystals were cryoprotected in a solution of 30% sucrose and 2.6 M ammonium sulfate and then flash-frozen in liquid nitrogen. The reflection was indexed, integrated, and scaled using the DPS/Mosflm software package (*17*, *18*). The space group was determined to be $P3_221$, with unit cell dimensions of $a = b = 73.3$ Å and $c = 99.4$ Å and one protein molecule per asymmetric unit. The statistics are summarized in Table 1.

Table 1: Data Collection and Processing

wavelength (Å)	1.0
temperature (K)	100.0
space group	$P3_221$
unit cell (Å)	$a = b = 73.3$, $c = 99.4$
resolution range (Å)	23.8−1.65 (1.74−1.65)[a]
observations	631678 (55893)
unique reflections	36271 (5246)
completeness (%)	100.0 (99.9)
average $I/\sigma(I)$	7.3 (6.0)
R_{merge}[b] (%)	7.2 (10.2)

[a] Values in parentheses refer to the highest resolution shell. [b] $R_{merge} = \sum_i|I_{av} - I_i|/\sum_i|I_i|$, where I_{av} is the average of all individual observations I_i.

Structure Determination. The initial model for refinement was the structure of the Toho-1 E166A mutant (PDB entry 1BZA) (*19*). The model was subjected to rigid body refinement, simulated annealing protocol with an initial temperature of 2000 K, positional minimization, and individual *B* factor refinement using the CNS software package (*20*). Manual model building was performed with O (*21*). The stereochemical quality of the model was monitored periodically using the program Procheck (*22*). After modeling of the protein structure, water molecules were automatically picked out using CCP4 (*23*). Sulfate ions were modeled into the obvious tetrahedral-shaped electron density in the solvent.

Kinetic Assays. The following antibiotics and chemicals were used for kinetic assays. Benzylpenicillin ($\Delta\epsilon_{233} = -1140$ M^{-1} cm^{-1}), cephalothin ($\Delta\epsilon_{262} = -7660$ M^{-1} cm^{-1}), and cephaloridine ($\Delta\epsilon_{260} = -10200$ M^{-1} cm^{-1}) were purchased from Sigma Chemical Co. (St. Louis, MO); nitrocefin ($\Delta\epsilon_{482} = 10000$ M^{-1} cm^{-1}) was from Unipath Oxoid (Basingstoke, U.K.). Imipenem ($\Delta\epsilon_{278} = -5660$ M^{-1} cm^{-1}) and cefoxitin ($\Delta\epsilon_{270} = -8380$ M^{-1} cm^{-1}) were gifts from Banyu Pharmaceutical Co. Ltd. (Tokyo, Japan); moxalactam ($\Delta\epsilon_{275} = -7960$ M^{-1} cm^{-1}), cefcapene ($\Delta\epsilon_{262} = -8500$ M^{-1} cm^{-1}), S1090 ($\Delta\epsilon_{296} = -7760$ M^{-1} cm^{-1}), and S4661 ($\Delta\epsilon_{298} = -9540$ M^{-1} cm^{-1}) were from Shionogi & Co. (Osaka, Japan); cefdinir ($\Delta\epsilon_{310} = -5390$ M^{-1} cm^{-1}) and ceftizoxime ($\Delta\epsilon_{257} = -7500$ M^{-1} cm^{-1}) were from Fujisawa Pharmaceutical Co. (Osaka, Japan); cefotaxime ($\Delta\epsilon_{264} = -7250$ M^{-1} cm^{-1}) was from Aventis Pharma (Tokyo, Japan); piperacillin ($\Delta\epsilon_{232} = -1640$ M^{-1} cm^{-1}) was from Toyama Chemical Co. (Tokyo, Japan); meropenem ($\Delta\epsilon_{298} = -9530$ M^{-1} cm^{-1}) was from Sumitomo Pharmaceutical Co. (Osaka, Japan); cefpodoxime ($\Delta\epsilon_{261} = -8500$ M^{-1} cm^{-1}) was from Sankyo Co. (Tokyo, Japan); faropenem ($\Delta\epsilon_{305} = -2950$ M^{-1} cm^{-1}) was from Suntory (Tokyo, Japan); ceftadizime ($\Delta\epsilon_{265} = -10300$ M^{-1} cm^{-1}) and clavulanic acid were from GlaxoSmithKline K.K. (Tokyo, Japan); cefepime ($\Delta\epsilon_{267} = -9120$ M^{-1} cm^{-1}) was from Bristol Pharmaceutical Co. (Tokyo, Japan); aztreonam ($\Delta\epsilon_{318} = -650$ M^{-1} cm^{-1}) was from Eisai Co. (Tokyo, Japan); sulbactam was from Pfizer Pharmaceutical Inc. (Tokyo, Japan); tazobactam was from Taiho Pharmaceutical Co. (Tokyo, Japan). The structures of several antibiotics are shown in Figure 6.

Hydrolysis of β-lactam antibiotics was detected by monitoring the variation in the absorbance of β-lactam solution in 50 mM phosphate buffer (pH 7.0). All measurements were made on a Uvikon 860 spectrophotometer linked to a personal computer. The reaction was performed in a total volume of 500 μL at 30 °C. For dilution of the enzyme,

Table 2: Refinement Statistics

resolution range (Å^2)	20−1.65 (1.73−1.65)[a]
R factor[b] (%)	18.2 (20.5)
R_{free} factor[c] (%)	19.7 (23.2)
average *B* factors (Å^2)	
whole structure	11.1
main chain	8.0
side chain	11.2
solvent	21.0
rmsd from ideal values	
bonds (Å)	0.009
angles (deg)	1.40

[a] Values in parentheses refer to the highest resolution shell. [b] $R = \sum|F_o - F_c|/\sum|F_o|$, where F_o and F_c are the observed and calculated structure factor amplitudes. [c] $R_{free} = \sum|F_o - F_c|/\sum|F_o|$, calculated using a test data set of 10% of the total data randomly selected from the observed reflections.

BSA was added to the buffer in the final concentration of 20 μg/mL to prevent denaturation of the enzyme. The reaction is described by the model:

$$E + S \underset{k_{-1}}{\overset{k_{+1}}{\leftrightarrow}} ES \xrightarrow{k_{+2}} E{-}S^* \xrightarrow{k_{+3}} E + P$$

where E is the enzyme, S is the substrate, ES is the noncovalent Michaelis complex, E−S* is the acyl-enzyme intermediate, and P is the inactive degradation product of the substrate. The steady-state kinetic parameters were determined by analyzing the complete hydrolysis time courses as described by De Meester et al. (*24*) or using the Hanes linearization of the Michaelis−Menten equation. The characteristic steady-state parameters derived from the model are

$$k_{cat} = \frac{k_{+2}k_{+3}}{k_{+2} + k_{+3}}$$

and

$$K_m = \frac{k_{+3}K}{k_{+2} + k_{+3}}$$

where

$$K = \frac{k_{-1} + k_{+2}}{k_{+1}}$$

The progress curves were measured at least three times for each substrate, and reproducible results were obtained.

RESULTS

Structure Determination. The refined structure of the wild-type Toho-1 β-lactamase is well-defined except for the N-terminal methionine at position 26 inserted for overexpression. The amino acid numbering used in this study follows the consensus numbering of Ambler et al. (*2*). The secondary structural elements are labeled according to the notations used for the E166A mutant (*19*). The model includes 261 amino acid residues, 284 water molecules, and 8 sulfate ions. The final model is refined to an *R* factor of 18.2% and a R_{free} factor of 19.7% at 1.65 Å resolution. The refinement results are summarized in Table 2.

Overall Structure. The overall structure of wild-type Toho-1 consists of two domains: an α/β domain and an α domain, as seen for the other class A β-lactamases. The root-mean-square deviation (rmsd) values for Cα atoms of Toho-1 from other structure-solved enzymes are listed in Table 3. The structure is essentially the same as that of the Toho-1 E166A mutant (Figure 1). The rmsd value between wild-type Toho-1 and the E166A mutant is 0.274 Å for Cα atoms and 0.621 Å for all atoms. A difference is observed around residue 166, which is glutamate in the wild-type enzyme but alanine in the E166A mutant. In the wild-type enzyme, the Ω loop, which contains Glu166 and forms the bottom wall of the active site, moves outward slightly to widen the active site cavity. When the structures of the wild-type enzyme and the mutant are superimposed, the distance between Cα atoms is 0.54 Å at position 166, 0.79 Å at position 104, 0.75 Å at position 165, and 0.33 Å at position 170. The shift of the Ω loop is caused by steric constraint between Glu166 and the neighboring residues and by the existence of water molecules Wat41 and Wat185 near the carboxyl group of Glu166. In comparison with other structure-solved class A enzymes, the smallest Cα difference (rmsd of 0.706 Å) is observed between Toho-1 and *Proteus vulgaris* K1 β-lactamase, an ESBL that is highly homologous to Toho-1 with 70% identity in the amino acid sequence (*25*).

Alternative Conformations. Alternative conformations are assigned to the side chains of the residues at positions 73, 94, 146, 153, 197, 201, and 218. Lys73 is in the active site, being thoroughly conserved in all of the known class A enzymes (Figure 2a) (*1*, *2*). Arg94, Asp146, Arg153, Lys197, and Glu201 are on the protein surface of the α domain, far from the active site. Ser218 is positioned on the top edge of the active site cleft.

Two alternative conformations of the Lys73 side chain are designated as conformation 1 and conformation 2 (Figure 3). In conformation 1, the side chain of Lys73 points toward Glu166, with the Nζ atom hydrogen-bonded to Glu166 Oϵ1, Ser70 Oγ, Asn132 Oδ1, and a water molecule Wat185. In conformation 2, the ammonium group of Lys73 points toward the hydroxyl group of Ser130, with the Nζ atom hydrogen-bonded to Ser130 Oγ, Ser70 Oγ, and Asn132 Oδ1. Conformation 1 is predominant in Toho-1, with an occupancy of 0.70. The *B* factors of Lys73 side-chain atoms are not high, and even lower than the average *B* factor for all side chains, suggesting that Lys73 prefers to take either one of the two conformations observed in this structure, rather than to be completely flexible. In the Toho-1 E166A mutant structure, the Lys73 conformation is largely analogous to conformation 2 (Figure 4). It indicates that the existence of the glutamate at position 166 strongly affects the conformation of Lys73, with considerable interaction between these two residues. Comparison of the Toho-1 structure with other class A enzymes shows that the Lys73 side chain takes a conformation similar to conformation 2 in most class A β-lactamases (Table 3). The exceptions are *Staphylococcus aureus* PC1 β-lactamase and *P. vulgaris* K1 β-lactamase, which have Lys73 side chains in a conformation resembling conformation 1 (Figure 4) (*25*, *26*). In the case of *Bacillus licheniformis* 749/C β-lactamase, two β-lactamase molecules in an asymmetric unit exhibit slightly different Lys73 conformations, and the Lys73 side chain of molecule B takes a form more similar to conformation 1 than that of molecule

Table 3: Comparison of Lys73 Configuration for Toho-1 and Other Class A β-Lactamases

enzyme	identity[a] (%)	PDB[b]	rmsd (Å)[c]	distance to K73 Nζ (Å)[d]				
				S70 Oγ	S130 Oγ	N132 Oδ1	E166 Oϵ1	Wat185 O
Toho-1 (C1)[e]				2.71[h]	3.99	2.92[h]	2.75[h]	3.06[h]
Toho-1 (C2)[f]				2.93[h]	2.70[h]	3.06[h]	4.36	4.72
E166A		1BZA	0.274	2.92[h]	3.14[h]	2.76[h]		
K1[g]	71.5	1HZO (a)	0.706	2.77[h]	3.97	2.95[h]	2.91[h]	2.84[h]
MYC	44.3	1MFO	2.015	2.89[h]	3.27	2.98[h]	3.26	
PER-1	25.4	1E25	2.667	2.75[h]	3.62	2.68[h]	3.55	
PC1	35.1	3BLM	1.950	2.54[h]	3.71	2.69[h]	2.83[h]	3.86[h]
TEM-1	38.3	1BTL	2.101	2.90[h]	4.17	2.97	3.42	
SHV-1	39.3	1SHV	2.344	2.84[h]	3.82	3.28	3.28	
BLICH[g]	41.2	4BLM (a)	1.213	2.83[h]	3.13[h]	2.56[h]	3.37	
		4BLM (b)	1.218	2.52[h]	3.24[h]	2.58	3.08[h]	3.62
ALBS	42.0	1BSG	1.224	2.77[h]	3.28	2.85[h]	3.27	
BS3[g]	40.9	1I2S (a)	0.948	2.69[h]	3.08[h]	2.86[h]	3.42	
NMC-A	49.0	1BUE	1.470	2.88[h]	3.13[h]	2.79[h]	3.44	
SME-1[g]	46.9	1DY6 (a)	1.424	2.81[h]	3.04[h]	2.63[h]	3.37	

[a] To amino acid sequence of Toho-1 β-lactamase. [b] PDB entry code; letters in parentheses indicate the molecule coordinate used in distance measurement. [c] rmsd from Toho-1 for all Cα atoms. [d] Distance between Lys73 Nζ and S70 Oγ, S130 Oγ, N132 Oδ, E166 Oϵ1, and a water molecule corresponding to Wat185 O in Toho-1. [e] C1 denotes conformation 1 of the Lys73 side chain. [f] C2 denotes conformation 2 of the Lys73 side chain. [g] Enzymes with two molecules in an asymmetric unit according to X-ray structural analysis, where (a) denotes the structure of the A molecule and (b) denotes the structure of the B molecule in each coordinate file. Enzymes: E166A, Toho-1 E166A mutant; K1, ESBL from *P. vulgaris* K1; MYC, *Mycobacterium fortuitum*; PER-1, *Pseudomonas aeruginosa*; PC1, β-lactamase from *S. aureus* PC1; TEM-1, *E. coli*; SHV-1, *Klebsiella pneumoniae*; ALBS, *S. albus* G; BS3, *B. licheniformis* BS3; BLICH, *B. licheniformis* 749/C; NMC-A, carbenicillinase from *Enterobacter cloacae*; SME-1, *Serratia marcescens*. [h] Denotes the hydrogen-bonding distance between Lys73 Nζ and each atom.

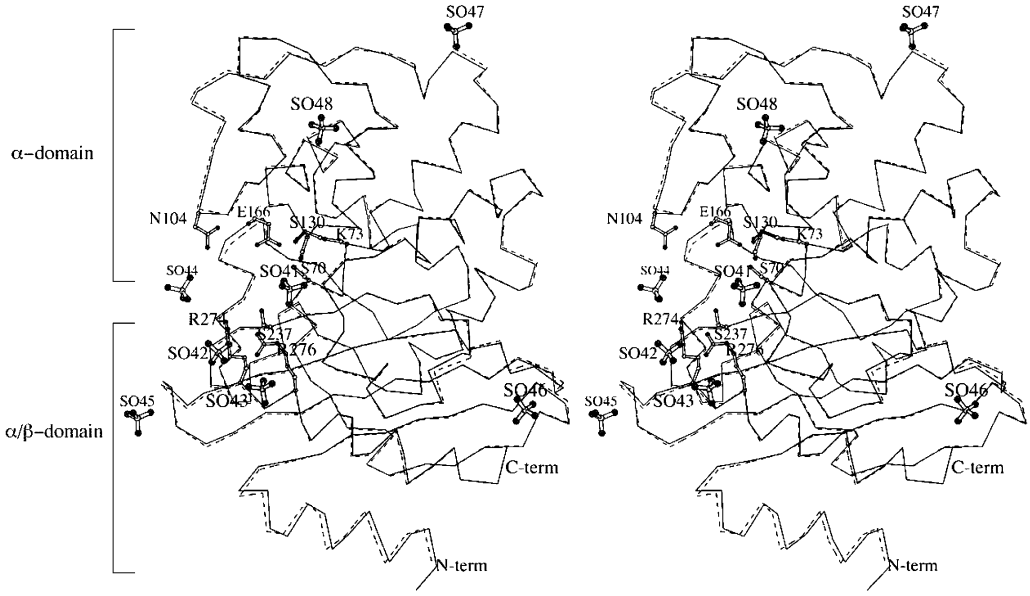

FIGURE 1: Stereoview of superimposed structures of wild-type Toho-1 and the E166A mutant. Bonds between Cα atoms in the wild-type enzyme are shown as solid lines, and those of the E166A mutant are shown as broken lines. Several residues mentioned in this study and the eight sulfate ions (SO41−SO48) observed in the wild-type enzyme are shown. The figure was generated using Molscript (*54*).

A (Figure 4) (*27*). The conformation of Lys73 is not necessarily correlated with any particular crystallization condition: Toho-1, the β-lactamase from *S. aureus* PC1, and the β-lactamase from *B. licheniformis* 749/C were all crystallized using ammonium sulfate as a precipitant, while the crystals of the β-lactamase from *P. vulgaris* K1 were obtained using PEG 6000. Similarly, no clear correlation was observed between the pH conditions for crystallization and the conformation of Lys73: Toho-1, *S. aureus* PC1 β-lactamase, *P. vulgaris* K1 β-lactamase, and *B. licheniformis* 749/C β-lactamase were crystallized at around pH 6.0, 8.5, 6.25, and 5.5, respectively. The β-lactamases listed in Table 3 were crystallized in a wide range of pH from 4.5 to 8.5.

The electron density map suggests that the side chains of Ser237 may also have alternative conformations. In the model, the hydroxyl group of Ser237 points into the active site cavity, hydrogen-bonding to the sulfate ion SO41 (Figure 3). Although the density is not clear enough to build a model for the second conformation, the map intimates that the side chain of Ser237 might rotate toward the N-terminal side of the B3 strand (Figure 2b).

Water Molecules in the Vicinity of Glu166. Two water molecules, Wat41 and Wat185, are located in positions close to the carboxyl group of Glu166, at distances from Glu166 Oϵ1 of 2.69 and 2.66 Å, respectively (Figure 3), though no hydrogen bonds are formed between Glu166 and these water

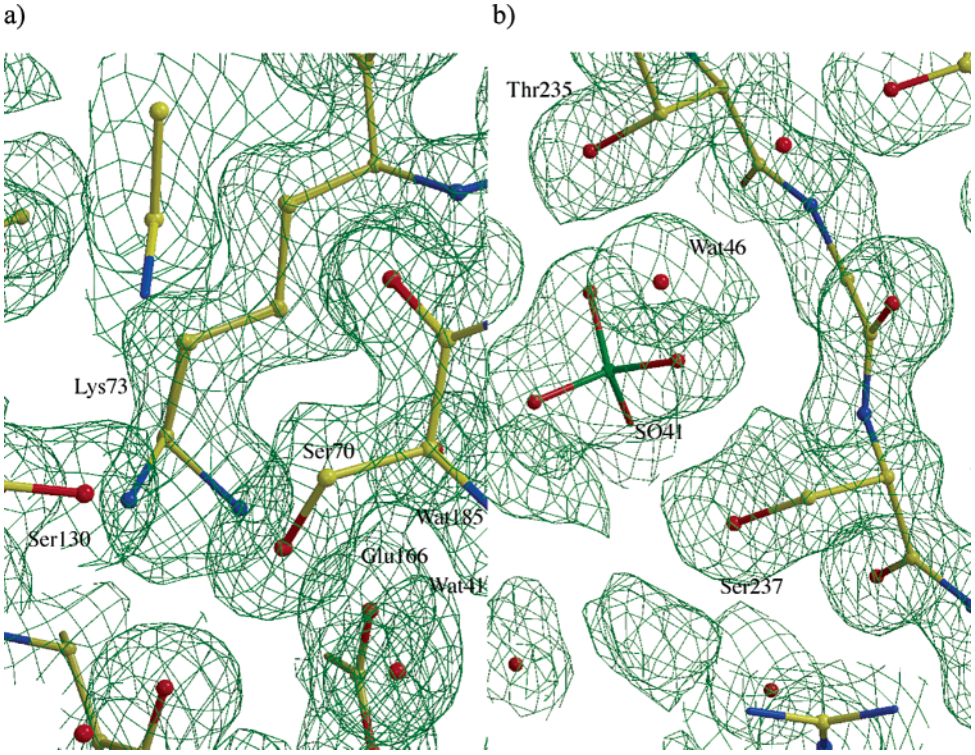

FIGURE 2: $2F_o - F_c$ electron density map around (a) Lys73 and (b) Ser237 at a contour level of 2σ. The map was calculated using the program CNS (*20*), omitting the side chain of Lys73 and Ser237. The figures were generated using Bobscript (*55*) and Raster3D (*56*, *57*).

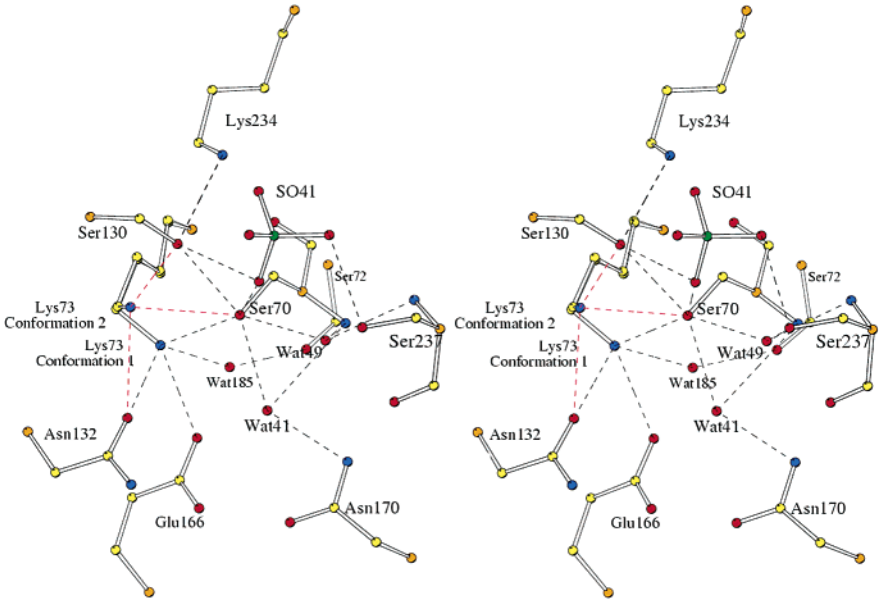

FIGURE 3: Stereoview of active site residues in the vicinity of Lys73. Hydrogen bonds are highlighted by dashed lines. Hydrogen bonds formed between Lys73 and other atoms in conformation 2 are indicated in red. The figure was generated using Molscript.

molecules. Wat41 is hydrogen-bonded to Ser70 Oγ, the backbone N of Ser70, and Asn170 Oδ1, and Wat185 is hydrogen-bonded to Ser72 Oγ and Nζ of Lys73 in conformation 1. No corresponding water molecules were observed in the structure of the E166A mutant, indicating the necessity of the Glu166 side chain to retain these water molecules. A water molecule corresponding to Wat41 exists in all the class A β-lactamase structures with the sole exception of Sme-1 and is regarded as a hydrolytic water molecule that is essential in the deacylation reaction (*25*−*34*). Among the class A enzymes, water molecules equivalent to Wat185 are only found in *S. aureus* PC1 β-lactamase, *P. vulgaris* K1 β-lactamase, and molecule B of *B. licheniformis* 749/C β-lactamase (*27*). In these enzymes, the conformation of the Lys73 side chain is identical or similar to conformation 1 (Figure 4). Thus, the second water molecule appears to require the Lys73 side chain to take conformation 1, in which the side chain is hydrogen-bonded to this water molecule.

Disposition of Sulfate Ions. Eight sulfate ions are modeled in the structure of Toho-1 (Figure 1). This model includes a much larger number of sulfate ions than the E166A mutant structure, in which only two sulfate ions are positioned. This difference is expected to follow simply from the difference in resolution or possibly from the difference in the quality

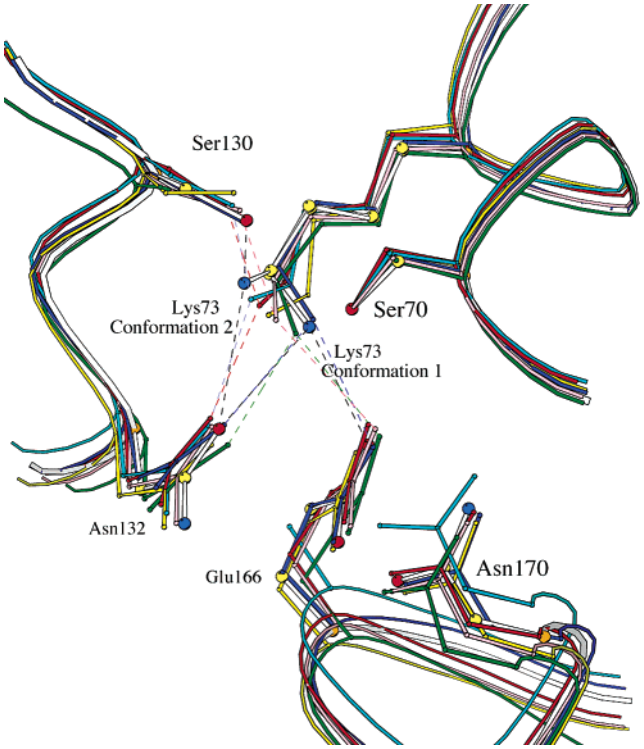

FIGURE 4: Comparison of Lys73 conformations. Structures of several enzymes listed in Table 3 are superimposed. The model of wild-type Toho-1 enzyme is depicted with the same color code as in Figure 3, with the E166A mutant rendered in cyan, β-lactamase from *P. vulgaris* K1 in blue, β-lactamase from *S. aureus* PC1 in green, TEM-1 in yellow, molecule A of *B. licheniformis* 749/C in red, and molecule B in pink. Hydrogen bonds formed between Lys73 Nζ and other residues are indicated by black broken lines for the wild-type Toho-1 enzyme and with broken lines of the corresponding color for other β-lactamases. The hydrogen bond between Lys73 Nζ and Ser70 Oγ was omitted in all structures for convenience.

of the crystals used for analysis. Of the eight sulfate ions, three sulfate ions, SO41, SO42, and SO43, are positioned in or near the active site cavity (Figures 1 and 5). SO41 is bound at the center of the active site, hydrogen-bonded to Ser70 Oγ, Ser130 Oγ, and Ser237 Oγ. In most structures of class A β-lactamases crystallized with ammonium sulfate as a precipitant, including the E166A mutant of Toho-1, a sulfate ion has been observed in the position equivalent to SO41 (*19*, *26*, *28*, *31*, *33*). Superimposing the Toho-1 structure on the structures of the acyl-enzyme complexes reveals that SO41 is in a position corresponding to the C3 (penicillins) or C4 (cephalosporins) carboxyl group of the substrates in the acyl-enzyme (*35*−*37*).

SO42 and SO43 are bound to the positively charged region formed by two arginine residues at positions 274 and 276 (Figure 5). Arg274 is unique to Toho-1, whereas the Arg/Lys residue at position 276 is highly conserved in the CTX-M-type enzymes (*28*, *38*).

Kinetic Study. The steady-state kinetic parameters k_{cat} and K_m were determined for a set of good β-lactam substrates (Table 4). The data indicated that the Toho-1 β-lactamase exhibited a broad-spectrum activity profile. The enzyme was active against both penicillins and cephalosporins. The best substrates of the Toho-1 β-lactamase were the first-generation cephalosporins such as cephalothin and cephaloridine. Cefotaxime was also a good substrate of Toho-1, but ceftazidime was poorly hydrolyzed by this enzyme. This can be attributed mainly to the large K_m value (K_m = 7.9 mM). Comparison of the kinetic constants of cephaloridine and ceftazidime indicates that the presence of a bulky carboxypropioxyimino group on the 7β lateral chain affects the efficiency of the β-lactamase. Interestingly, new β-lactam compounds such as cefdinir, cefcapene, cefepime, and S1090 (fourth-generation cephalosporins) behaved as good substrates of Toho-1. Among the mechanism-based inactivators, sulbactam was also a good substrate of Toho-1. Cefoxitin (a cephamycin) and moxalactam (an oxacephem) were poor substrates, and interaction with Toho-1 led to the formation of a rather stable acyl enzyme, characterized by a deacylation-limiting step and by low acylation efficiency (k_2/K < 800 M^{-1} s^{-1}) (Table 5). All tested carbapenems behaved as poor substrates of Toho-1, with meropenem exhibiting the highest acylation efficiency ($k_2/K = 10^5$ M^{-1} s^{-1}). Interestingly, all deacylation rate constants and K_m values were very low. Finally, tazobactam behaved as a poor inactivator of Toho-1, with an acylation efficiency of 450 M^{-1} s^{-1}.

Table 4: Kinetic Parameters of Toho-1 against Various Antibiotics

class (generation)[a]	antibiotic	k_{cat} (s^{-1})	K_m (μM)	k_{cat}/K_m ($\mu M^{-1} s^{-1}$)
penicillin	benzylpenicillin	68	23	3.0
	piperacillin	13	8.0	1.7
cephalosporin (1)	nitrocefin[b]	160	59	2.7
	cephaloridine	200	280	0.7
	cephalothin	480	39	12
cephalosporin (3)	cefotaxime	250	120	2.1
	ceftazidime	21	7900	0.0013
	ceftizoxime	ND	ND[c]	0.12
	cefpodoxime	ND	ND[c]	0.11
cephalosporin (4)	cefepime	ND	ND[c]	0.068
	cefdinir	2.1	1.4	1.5
	cefcapene	100	46	2.2
	S1090	21	3.8	5.5
inhibitor	sulbactam	0.18	0.31	0.58

[a] Generation of cephalosporins is indicated in parentheses. [b] Classified as first generation according to structure. [c] Too high to determine.

Table 5: Kinetic Parameters of Toho-1 against Poor Substrates and Inhibitors

class[a]	antibiotics	K_{cal}[b] (μM)	k_{+2} (s^{-1})	k_{+3} (s^{-1})	k_{+2}/K ($M^{-1} s^{-1}$)
cephamycin	cefoxitin	8	ND	6.1×10^{-3}	760
oxacephem	moxalactam	20	ND	5.0×10^{-3}	250
carbapenem	imipenem	2.4[c]	ND	5.6×10^{-3}	2250
	meropenem	0.09[c]	ND	8.9×10^{-3}	1.0×10^5
	faropenem	0.01	ND	9.6×10^{-3}	1900
	S4661	0.36	ND	4×10^{-3}	1.1×10^4
inhibitor	tazobactam	ND	ND	ND	450

[a] Generation for cephems. [b] K calculated from measured values. [c] Measured as K_i value in competition experiments.

DISCUSSION

Alternative Conformations of Lys73. As a whole, the active site structure of Toho-1 is quite similar to that of other class A β-lactamases. The most significant exception is the conformation of Lys73. The present structural analysis revealed the existence of alternative conformations of Lys73 for the first time among class A β-lactamases. Although a number of previous structural and mutagenesis studies have indicated that Lys73 is expected to play a critical role in

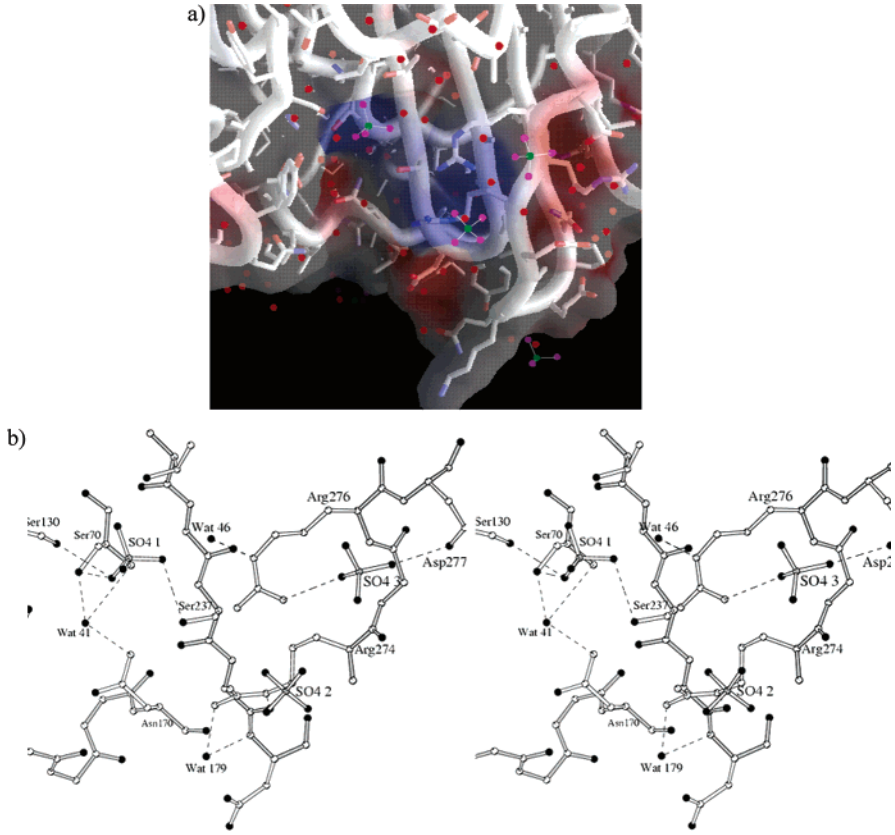

FIGURE 5: Sulfate ions binding near the active site. (a) Surface representation of the active site cleft. The transparent surface is colored according to the electrostatic potential from −30 kT (red) to +30 kT (blue). Backbones of the protein are shown as coils, and side chains within 1.5 Å of the protein surface are indicated. Water molecules are depicted in red, and sulfate ions are illustrated with green S atoms and magenta O atoms. (b) Stereoview of sulfate ion binding site near the catalytic cleft. Hydrogen bonds are indicated by dashed lines. The surface potential was calculated by GRASP (*58*).

catalysis, the role of Lys73 remains unclear (*3*, *39*). Kinetic analysis of the K73R mutant of *Bacillus cereus* 569/H β-lactamase I and the K73A mutant of *B. licheniformis* β-lactamase showed that Lys73 was involved both in acylation and in deacylation (*40*, *41*), and it was concluded that Lys73 would work to maintain an optimum electrostatic environment for fully efficient catalytic reaction, not as a general base. On the other hand, structural analysis of the acyl-enzyme suggested the role of Lys73 as a candidate of the general base to accept a proton from Ser70 prior to acylation (*35*). To function as a general base, Lys73 should be in an unprotonated state; however, the protonation state of this residue remains controversial (*42*, *43*).

The role of Glu166 in acylation is also uncertain, while it is known to act as a general base in deacylation (*35*, *44*). Precise mutagenesis studies showed that the replacement of Glu166 caused a drastic decrease in both the acylation and deacylation rates (*39*, *40*, *45*). The high-resolution structure of TEM-1 β-lactamase complexed with an acylation transition-state analogue revealed that the Glu166 side chain was protonated, which proposed that Glu166 activated Ser70 via a catalytic water molecule in acylation (*46*). Through structural analysis of the E166A mutant of *B. licheniformis* β-lactamase, it was found that removal of the Glu166 side chain did not change the conformation of Lys73. It suggested the existence of no strong salt bridge between Glu166 and Lys73, precluding the possibility of proton transfer between the two in the acylation process (*47*). In Toho-1, removal of the Glu166 side chain changes the position of Lys73 significantly. Conformation 1 of Lys73 indicates possible proton transfer between Lys73 and Glu166; conformation 2, between Lys73 and Ser130. Considering the present structural analysis and the results of previous studies, we speculate that there are several proton-relay pathways in acylation and that Lys73 would be involved in proton transfer in at least some of these pathways. Two possible speculated proton-transfer pathways in acylation are as follows: (1) after proton transfer from the Lys73 ammonium group to the Glu166 carboxylate, the unprotonated Lys73 would act as a general base to activate Ser70, or (2) the substrate carboxylate oxygen would accept a proton from the hydroxyl group of Ser130, which, then unprotonated, would accept a proton from Lys73, and finally the neutralized Lys73 would activate Ser70, as proposed by Ishiguro et al. (*48*). Proton relay involving Ser130 might represent a secondary pathway, or a water molecule might substitute for Ser130. This follows from the observation that mutants of the *Streptomyces albus* G enzyme with Ser130 replaced with alanine or glycine retained significant activity (*49*). Although this structural analysis has indicated the possibility of various proton-transfer pathways in catalysis, further research that directly shows the protonation state of these residues in each step of catalysis will be necessary before any concrete conclusions can be drawn.

The difference in Lys73 conformation observed among the structure-solved β-lactamases might reflect some subtle but significant differences in the active site properties (Table 3). The conformation of Lys73, together with the existence of the second water molecule in the active site, implies that Toho-1, *P. vulgaris* K1 β-lactamase, *S. aureus* PC1 β-lac-

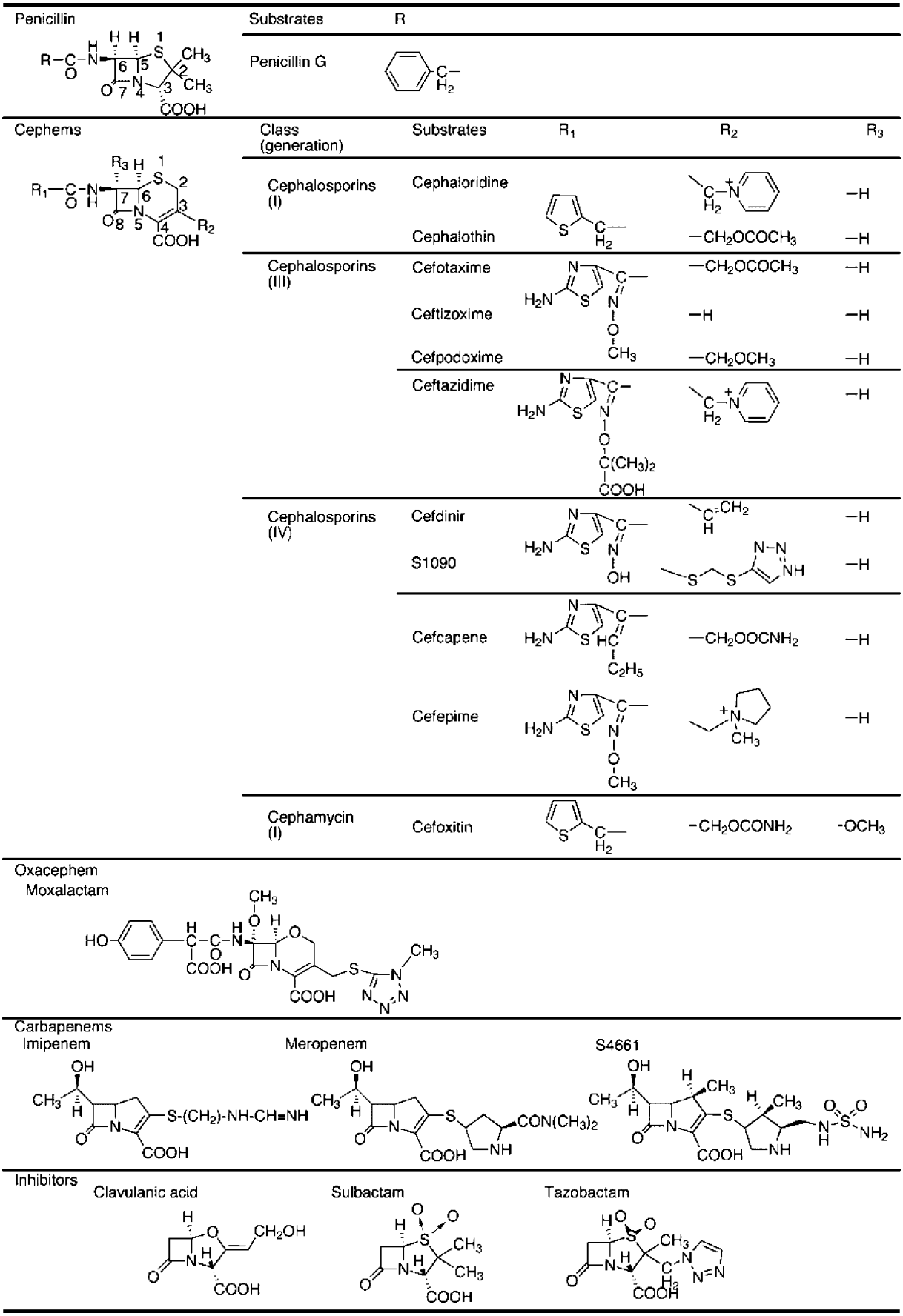

FIGURE 6: Structures of selected β-lactam antibiotics used in this study.

tamase, and possibly *B. licheniformis* β-lactamase share a common active site environment. As the β-lactamase from *P. vulgaris* K1 is an ESBL highly homologous to Toho-1, one of the necessary conditions for extending the substrate

specificity of CTX-M-type ESBLs might be to maintain conformation 1 of Lys73, although this could not be the sole condition.

The Role of Water Molecules in the Vicinity of Glu166. From the comparison of the structures between wild-type Toho-1 and the E166A mutant, we speculate that Glu166 is necessary to retain Wat41 and Wat185, though there is no hydrogen bond formation between Glu166 and these water molecules. We presume that the existence of glutamate at position 166 might affect the active site environment to retain these water molecules. Since the distance between Glu166 and these water molecules is sufficiently short, a slight movement of Glu166 and/or water molecules might be sufficient to form the hydrogen bonds, thus allowing Glu166 and these water molecules to participate in the proton transfer.

The Role of Ser237. In the Toho-1 structure, the hydroxyl group of Ser237 points into the active site cavity. It is hydrogen-bonded to sulfate ion SO41, which is suggested to correspond to the C3 (penicillins) or C4 (cephalosporins) carboxylate group of β-lactam antibiotics. This interaction is suggestive of the direct participation of Ser237 in substrate binding. Position 237 is occupied by alanine in many class A β-lactamases but is populated with serine or threonine in the CTX-M-type β-lactamases, carbenicillinases, and several other β-lactamases (*28*, *38*). The crystal structures of several enzymes with Ser/Thr at position 237 have been solved, and in all of these structures except Toho-1, it is found the hydroxyl group of Ser237 points toward the direction of the N-terminus of the B3 strand, not toward the active site. For example, the Ser237 side chain of *P. vulgaris* K1 β-lactamase is hydrogen-bonded to water molecule Wat547 over β-sheet B3. In the carbapenemases Sme-1 and NMC-A, the hydroxyl group of Ser237 is hydrogen-bonded to the side chain of Arg220, which is a site often occupied by a serine residue in CTX-M-type enzymes (*29*, *30*). The unique conformation of Ser237 observed in Toho-1 appears to be caused by the existence of sulfate ion SO41 bound in the center of the active site, which is absent in the other structure-solved enzymes with Ser/Thr at position 237. From comparison of the crystal structures and the corresponding crystallization conditions, the side chain of Ser237 is considered to rotate as the sulfate ion and possibly substrate bind to the catalytic site. The S237A mutant of *P. vulgaris* K1 β-lactamase has been shown to retain its penicillinase activity, whereas the cephalosporinase activity, particularly for oxyimino cephalosporins, decreased dramatically, mainly due to the decrease in k_{cat} (*50*). Taken together, the hydroxyl group of Ser237 is hypothesized to be hydrogen-bonded to the C3 (penicillins) or C4 (cephalosporins) carboxyl group of substrate in the formation of the Michaelis complex and to change conformation as the carboxylate of the substrate changes position. The hydroxyl group might be involved in the exact positioning of the substrates in the hydrolytic reaction, particularly oxyimino cephalosporins. In the hydrolysis of carboxypropylimino cephalosporins, the carboxyproxylimino group might inhibit the proper functioning of Ser237, resulting in the apparently small k_{cat} and large K_m obtained in kinetic analysis.

Disposition of Sulfate Ions. The structural analysis of Toho-1 reveals that SO42 and SO43 are bound to the positively charged region formed by two arginine residues, Arg274 and Arg276 (Figure 5). Toho-1 mutants with Arg274 and/or Arg276 replaced with nonpositively charged residues exhibited an approximately 50% decrease in k_{cat}/K_m for the third-generation cephems, yet without obvious change for penicillins and first-generation cephems (unpublished data). The substitution of asparagine for arginine at position 276 of the ESBL CTX-M-4 resulted in lower resistance to oxyimino cephalosporins, whereas the level of resistance to penicillins remained unchanged (*51*). Considering these results and the fact that the arginine residue at position 276 is highly conserved in CTX-M-type enzymes, this positively charged region is speculated to function as a pseudo-substrate-binding site that would interact with the methoxyimino group of cefotaxime and other third-generation cepharosporins prior to binding in the active site. This region may also help to lead the substrate into the final binding position or facilitate binding to the active site.

Substrate Profile of Toho-1. It is the characteristic of Toho-1 and other CTX-M-type ESBLs to hydrolyze third-generation cephalosporins effectively (*9*−*15*). Toho-1 hydrolyzes ceftazidime far less efficiently than third-generation cephalosporins with a methoxyimino group in the 7β side chain. The size and constitution of the 7β side chain therefore appear to be critical in the processes of substrate binding and hydrolysis. The bulky carboxypropoxyimino group in the 7β side chain may cause steric conflict or unfavorable electrostatic interaction and/or repulsion with the enzyme.

Toho-1 exhibited very low activity for cefoxitin, a second-generation cephamycin, probably due to the 7α-methoxy group. As shown in the structural analysis of the β-lactamase from *B. licheniformis* BS3, the 7α-methoxy group would cause a conformational change of the 7β side chain, eliminating the hydrolytic water molecule and changing the conformation of the Ω loop, both essential in hydrolysis (*52*). Moxalactam, an oxacephem with a 7α-methoxy group, might also react in a similar fashion, resulting in the accumulation of acyl intermediates and thus inactivation of the enzyme.

Toho-1 exhibited high affinity and detectable activity against carbapenems, with small K_i and k_{cat} values. This suggests the possibility that Toho-1-like enzymes acquire higher carbapenemase activity with evolution. In the structures of carbapenemases NMC-A and Sme-1, several unique features differing from Toho-1 and other class A β-lactamases are observed. First, a disulfide bridge exists between Cys69 and Cys238, resulting in reorientation of the main-chain carbonyl O atom at position 238 toward the active site cavity. This disulfide bridge has been shown through analysis of the Cys69Ala mutant to be critical in catalysis and/or structural stability, as indicated by the full susceptibility of the strain producing the mutant to imipenem and all other antibiotics (*29*). Second, possibly as a consequence of the disulfide bond, the main-chain conformation from residue 238 to residue 240 in the β-strand B3 differs markedly from that of other class A enzymes, resulting in an increase in the space available between the Ω loop and the B3 strand. Third, the hydroxyl group of Ser237 points toward the ammonium group of Arg220, which is well conserved in carbapenemases. The Ser237 Ala mutant of Sme-1 exhibited significantly lower activity against imipenem (*53*), indicating that this conformation of Ser237 might be critical in carbapenemase activity. Mutation would occur in these regions if Toho-1-type enzymes obtained higher carbapenem-

hydrolyzing activity, although it is still not clear how these structural features are correlated with carbapenemase activity.

β-Lactamase inhibitors such as clavulanic acid, sulbactam, and tazobactam are known mechanism-based inactivators of class A enzymes. The k_{cat} value for sulbactam could be calculated, and the MIC value for sulbactam/cefoperazone was not small (data not shown). Toho-1 therefore appears to have acquired resistance against sulbactam. Toho-1 mutants with stronger resistance against sulbactam and other inhibitors might appear in the future.

ACKNOWLEDGMENT

Thanks are extended to Professor N. Sakabe and the staff of the Photon Factory, KEK, Tsukuba, for kind help with data collection and data processing and to Professor S. Iwata of Imperial College, London, for advice on structure refinement.

REFERENCES

1. Matagne, A., Dubus, A., Galleni, M., and Frère, J.-M. (1999) *Nat. Prod. Rep. 16*, 1−19.
2. Ambler, R. P., Coulson, A. F. W., Frère, J.-M., Ghuysen, J.-M., Joris, B., Forsman, M., Levesque, R. C., Tiraby, G., and Waley, S. G. (1991) *Biochem. J. 276*, 269−272.
3. Matagne, A., Lamotte-Brasseur, J., and Frère, J.-M. (1998) *Biochem. J. 330*, 581−598.
4. Du, B. S., Marriott, M. S., and Amyes, S. G. (1995) *J. Antimicrob. Chemother. 35*, 7−22.
5. Knox, J. R. (1995) *Antimicrob. Agents Chemother. 39*, 2593−2601.
6. Petrosino, J., Cantu, C., III, and Palzkill, T. (1998) *Trends Microbiol. 6*, 323−327.
7. Orencia, M. C., Yoon, J. S., Ness, J. E., Stemmer, W. P. C., and Stevens, R. C. (2001) *Nat. Struct. Biol. 8*, 238−242.
8. Majiduddin, F. K., and Palzkill, T. (2003) *Genetics 163*, 457−466.
9. Tzouvelekis, L. S., Tzelepi, E., Tassios, P. T., and Legakis, N. J. C. (1999) *Int. J. Antimicrob. Agents 14*, 137−142.
10. Ishii, Y., Ohno, A., Taguchi, H., Imajo, S., Ishiguro, M., and Matsuzawa, H. (1995) *Antimicrob. Agents Chemother. 39*, 2269−2275.
11. Bonnet, R., Dutour, C., Sampaio, J. L., Chanal, C., Sirot, D., Labia, R., De, C. C., and Sirot, J. (2001) *Antimicrob. Agents Chemother. 45*, 2269−2275.
12. Poirel, L., Naas, T., Thomas, I. L., Karim, A., Gingen, E., and Nordmann, P. (2001) *Antimicrob. Agents Chemother. 45*, 3355−3361.
13. Ma, L., Ishii, Y., Ishiguro, M., Matsuzawa, H., and Yamaguchi, K. (1998) *Antimicrob. Agents Chemother. 42*, 1181−1186.
14. Yagi, T., Kuroskawa, H., Senda, K., Ichiyama, S., Ito, H., Ohsuka, S., Shibayama, K., Shimokawa, K., Kato, N., Ohta, M., and Arakawa, Y. (1997) *Antimicrob. Agents Chemother. 41*, 2606−2611.
15. Bradford, P. A., Yang, Y., Sahm, D., Grope, I., Gardovska, D., and Storch, G. (1998) *Antimicrob. Agents Chemother. 42*, 1980−1984.
16. Bush, K., Jacoby, G. A., and Medeiros, A. A. (1995) *Antimicrob. Agents Chemother. 39*, 1211−1233.
17. Steller, I., Bolotovsky, R., and Rossmann M. G. (1997) *J. Appl. Crystallogr. 30*, 1036−1040.
18. Bolotovsky, R., Steller, I., and Rossmann M. G. (1998) *J. Appl. Crystallogr. 31*, 708−717.
19. Ibuka, A., Taguchi, A., Ishiguro, M., Fushinobu, S., Ishii, Y., Kamitori, S., Okuyama, K., Yamaguchi, K., Konno, M., and Matsuzawa, H. (1999) *J. Mol. Biol. 285*, 2079−2087.
20. Brunger, A. T., Adams, P. D., and Clore, G. M. (1998) *Acta Crystallogr. D54*, 905−921.
21. Jones, T. A., and Kjeldgaard, M. (1995) *Manual for O version 5.10*, Uppsala, Sweden.
22. Laskowski, R. A., MacArthur, M. W., Moss, D. S., and Thornton, J. M. (1993) *J. Appl. Crystallogr. 26*, 283−291.
23. Collaborative Computational Project, Number 4 (1994) *Acta Crystallogr. D50*, 760−763.
24. De Meester, F., Joris, B., Reckinger, G., Bellefroid-Bourguignon, C., Frère, J.-M., and Waley, S. G. (1987) *Biochem. Pharmacol. 36*, 2393−2403.
25. Nukaga, M., Mayama, K., Crichlow, G. V., and Knox, J. R. (2002) *J. Mol. Biol. 317*, 109−117.
26. Herzberg, O., and Moult, J. (1987) *Science 236*, 694−701.
27. Moews, P. C., Knox, J. R., Dideberg, O., Charlier, P., and Frère, J.-M. (1990) *Proteins 7*, 156−171.
28. Tranier, S., Bouthors, A. T., Maveyraud, L., Guillet, V., Sougakoff, W., and Samama, J. P. (2000) *J. Biol. Chem. 275*, 28075−28082.
29. Sougakoff, W., L'Hermite, G., Pernot, L., Naas, T., Guillet, V., Nordmann, P., Jarlier, V., and Delettre, J. (2002) *Acta Crystallogr. D58*, 267−274.
30. Swaren, P., Maveyraud, L., Raquet, X., Cabantous, S., Duez, C., Pedelacq, J. D., Mariotte-Boyer, S., Mourey, L., Labia, R., Nicolas-Chanoine, M. H., Nordmann, P., Frère, J.-M., and Samama, J. P. (1998) *J. Biol. Chem. 273*, 26714−26721.
31. Jelsch, C., Mourey, L., Masson, J. M., and Samama, J. P. (1993) *Proteins 16*, 364−383.
32. Kuzin, A. P., Nukaga, M., Nukaga, Y., Hujer, A. M., Bonomo, R. A., and Knox, J. R. (1999) *Biochemistry 38*, 5720−5727.
33. Dideberg, O., Charlier, P., Wery, J. P., Dehottay, P., Dusart, J., Erpicum, T., Frère, J.-M., and Ghuysen, J.-M. (1987) *Biochem. J. 245*, 911−913.
34. Lim, D., Sanschagrin, F., Passmore, L., De Castro, L., Levesque, R. C., and Strynadka, N. C. (2001) *Biochemistry 40*, 395−402.
35. Strynadka, N. C., Adachi, H., Jensen, S. E., Johns, K., Sielecki, A., Betzel, C., Sutoh, K., and James, M. N. (1992) *Nature 359*, 700−705.
36. Chen, C. C., and Herzberg, O. (2001) *Biochemistry 40*, 2351−2358.
37. Fonze, E., Vanhove, M., Dive, G., Sauvage, E., Frère, J.-M., and Charlier, P. (2002) *Biochemistry 41*, 1877−1885.
38. Bonnet, R., Sampaio, J. L., Chanal, C., Sirot, D., De Champs, C., Viallard, J. L., Labia, R., and Sirot, J. (2000) *Antimicrob. Agents Chemother. 44*, 3061−3068.
39. Matagne, A., and Frère, J.-M. (1995) *Biochim. Biophys. Acta 1246*, 109−127.
40. Gibson, R. M., Christensen, H., and Waley, S. G. (1990) *Biochem. J. 272*, 613−619.
41. Lietz, E. J., Truher, H., Kahn, D., Hokenson, M. J., and Fink, A. L. (2000) *Biochemistry 39*, 4971−4981.
42. Damblon, C., Raquet, X., Lian, L. Y., Lamotte-Brasseur, J., Fonze, E., Charlier, P., Roberts, G. C., and Frère, J.-M. (1996) *Proc. Natl. Acad. Sci. U.S.A. 93*, 1747−1752.
43. Swaren, P., Maveyraud, L., Guillet, V., Masson, J. M., Mourey, L., and Samama, J. P. (1995) *Structure 3*, 603−613.
44. Adachi, H., Ohta, T., and Matsuzawa, H. (1991) *J. Biol. Chem. 266*, 3186−3191.
45. Guillaume, G., Vanhove, M., Lamotte-Brasseur, J., Ledent, P., Jamin, M., Joris, B., and Frère, J.-M. (1997) *J. Biol. Chem. 272*, 5438−5444.
46. Minasov, G., Wang, X., and Shoichet, B. K. (2002) *J. Am. Chem. Soc. 124*, 5333−5340.
47. Knox, J. R., Moews, P. C., Escobar, W. A., and Fink, A. L. (1993) *Protein Eng. 6*, 11−18.
48. Ishiguro, M., and Imajo, S. (1996) *J. Med. Chem. 39*, 2207−2218.
49. Jacob, F., Joris, B., Lepage, S., Dusart, J., and Frère, J.-M. (1990) *Biochem. J. 271*, 399−406.
50. Tamaki, M., Nukaga, M., and Sawai, T. (1994) *Biochemistry 33*, 10200−10206.
51. Gazouli, M., Legakis, N. J., and Tzouvelekis, L. S. (1998) *FEMS Microbiol. Lett. 169*, 289−293.
52. Fonze, E., Vanhove, M., Dive, G., Sauvage, E., Frère, J.-M., and Charlier, P. (2002) *Biochemistry 41*, 1877−1885.
53. Sougakoff, W., Naas, T., Nordmann, P., Collatz, E., and Jarlier. V. (1999) *Biochim. Biophys. Acta 1433*, 153−158.
54. Kraulis, P. (1991) *J. Appl. Crystallogr. 24*, 946−950.
55. Esnouf, R. M. (1997) *J. Mol. Graphics 15*, 132−134.
56. Bacon, D. J., and Anderson, W. F. (1988) *J. Mol. Graphics 6*, 219−220.
57. Merritt, E. A., and Murphy, M. E. P. (1994) *Acta Crystallogr. D50*, 869−873.
58. Nayal, M., Hitz, B. C., and Honig, B. (1999) *Protein Sci. 8*, 676−679.

BI0342822